EAST EUROPEAN JOURNAL OF PHYSICS. **2.** 258-266 (2025)
DOI:10.26565/2312-4334-2025-2-31 ISSN 2312-4334

i-ZnO AND CdS BUFFER LAYERS FOR IMPROVING THE EFFICIENCY OF COPPER TIN SULPHIDE QUANTUM DOT SENSITIZED SOLAR CELLS

Maya Mathew*
Department of Physics, Carmel College (Autonomous), Mala, Thrissur, Kerala, India
**Corresponding Author Email: maya@carmelcollegemala.ac.in*
Received February 24, 202; revised April 17, 2025; accepted April 30, 2025

The effect of layer defects as well as interface defects in copper tin sulphide quantum dot sensitized solar cells were investigated using SCAPS-1D software. Layer defects in the sensitizer and hole transporting layer were found to have no effect on the cell efficiency except at very high densities of 10^{19} cm^{-2}. The interface defect at CTS/ETL was also found to have no effect on the cell efficiency. Defects at the HTL/CTS interface decreased the cell efficiency significantly and so a buffer layer was introduced at this interface. Both i-ZnO and CdS buffer layer materials were found to have energy levels in alignment with the HTL enhancing charge transport. The cell efficiency increased from 17.86% to 18.37% with i-ZnO buffer layer while the cell efficiency rose to 18.61% when CdS was used as the buffer layer. Absorption of the solar spectrum in the blue-green region was enhanced when buffer layers were used in the cell.
Keywords: *Quantum dot sensitized solar cells; Buffer layer; SCAPS-1D; Charge carrier recombination; Quantum efficiency; Defects*
PACS: 61.46.+w., 61.72.Ww., 73.21.La., 73.50.Pz

1. INTRODUCTION

Quantum dot sensitized solar cells are being extensively researched now-a-days due to several characteristic phenomena in quantum dots such as quantum confinement, multiple electron generation, high absorption coefficient and cost effectiveness [1-3]. Quantum confinement is a quantum phenomenon in which the bandgap of the material can be tuned according to its size. This fine tuning of bandgap is possible only if the size of the particle is less than the Bohr radius of charge carriers, i.e., the average distance between the electron and a hole in an exciton [4-6]. Multiple electron generation is another quantum phenomenon in which a high energy photon can excite more than one electron. Quantum dots naturally have high absorption coefficients which make them potential candidates in solar cells [7-9]. Quantum dots are now being prepared by simple deposition techniques such as colloidal synthesis [10] and successive ionic layer adsorption and reaction techniques and that too at room temperature [11,12], which can bring down the cost of making a solar cell. This work is on copper tin sulphide (CTS) quantum dots sensitized solar cells where CTS is a ternary semiconductor with high absorption coefficient of 10^4 cm^{-1}. Quantum dots of CTS have been prepared by solvothermal, hydrothermal and ball milling techniques and cost effective and room temperature techniques too such as colloidal synthesis and SILAR techniques [13-18].

Quantum dot sensitized solar cells are similar to dye sensitized solar cells where the dye has been replaced by the sensitizer which are quantum dots. The quantum dots are usually coated onto a porous electron transporting layer (ETL) and transparent conducting oxides are the electrical contacts for taking the charge carriers out of the solar cell. The hole transporting layer (HTL) allows the extraction of holes from the sensitizer to the electrical contacts [19, 20].

Similar to the various types of defects present in solar cells leading to charge carrier recombination, QDSSCs also have various types of defects [21, 22]. There can be defects within the layers of sensitizer, affecting photon absorption, defects in the HTL, affecting hole transport and also interface defects where the recombination happens between different layers. Investigation on the effect of various defects in the solar cell is very important for improving the efficiency of the solar cell. Buffer layers are inserted between the layers where interface recombination is more and the cell efficiency is enhanced. Commonly used buffer layers are ZnS, ZnO, i-ZnO, CdS and CdSe. Buffer layers are so chosen that their valence band is in alignment with that of the HTL, facilitating the hole transport [23- 25].

ZnS buffer when used in CTS thin film solar cells, decreased the interface recombination and enhanced the cell efficiency by 1% compared to the CdS buffer layer [26]. Ag_2S quantum dots and also that in bulk were found to be good buffer layers in CIGS solar cells. It was found that not only the band alignment but also the opto-electrical properties of the buffer layer affect the efficiency of the solar cell. Higher bandgap and higher carrier concentration buffer layers improve the power conversion efficiency of the device [27]. Decrease in charge carrier recombination at the CdTe quantum dots absorber layer and the metal oxide layer were observed when ZnS buffer layer was used and the cell efficiency was found to improve by 2% [28].

In this work, the effect of layer as well interface defects in CTS QDSSCs are investigated and then a comparison between i-ZnO and CdS buffer layers have been made. This is a first approach made in the study of the effect of the buffer layer in CTS QDSSCs.

Cite as: M. Mathew, East Eur. J. Phys. 2, 258 (2025), https://doi.org/10.26565/2312-4334-2025-2-31

2. DESIGN AND SIMULATION

Copper Tin sulphide quantum dot sensitized solar cell having the structure ITO/TiO_2/CTS/$CuSbS_2$/Au was simulated where, ITO is the transparent conducting oxide, TiO_2 is the electron transporting layer, CTS quantum dots of bandgap 2.5 eV is the sensitizer layer, $CuSbS_2$ is the hole transporting layer and Au is the metal back contact with a workfunction of 5.1 eV. The schematic diagram of the solar cell as well as its band structure has been shown in Figures 1 and 2 respectively.

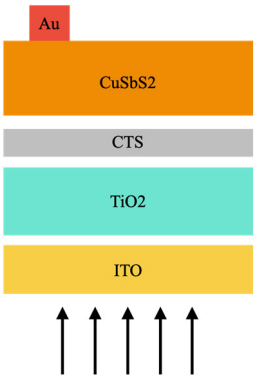

Figure 1. Solar cell structure used for simulation

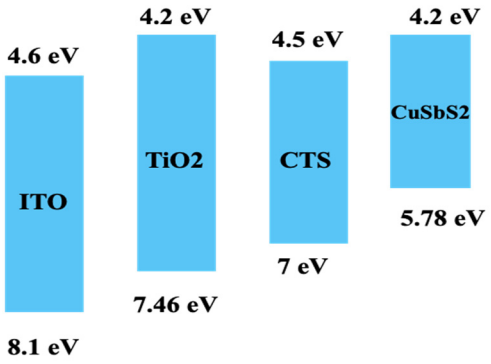

Figure 2. Band structure for the solar cell ITO/TiO_2/CTS/$CuSbS_2$/Au

This QDSSC was optimized previously for all the layer parameters and accordingly the layer thicknesses, doping densities and defect densities were taken. The layer parameters have been tabulated in Table 1.

Table 1. Layer parameters used in simulation of the solar cell structure

Parameters	ITO	TiO_2	CTS	$CuSbS_2$
Thickness (μm)	0.05	0.3	0.01	1
Bandgap Eg (eV)	3.5	3.26	2.5	1.58
Electron affinity (eV)	4.6	4.2	4.5	4.2
Dielectric constant ($\varepsilon/\varepsilon_0$)	8.9	10	10	14.6
Density of state conduction band (cm^{-3})	2.2×10^{18}	2.0×10^{17}	1×10^{19}	2×10^{18}
Density of state valence band (cm^{-3})	1.8×10^{19}	6×10^{17}	1×10^{19}	1×10^{18}
Thermal velocity of electron V_e (cms^{-1})	1×10^{7}	1×10^{7}	1×10^{7}	1×10^{7}
Thermal velocity of holes V_h (cms^{-1})	1×10^{7}	1×10^{7}	1×10^{7}	1×10^{7}
electron mobility μ_e (cm^2/V_s)	10	100	100	49
hole mobility μ_h (cm^2/V_s)	10	250	25	49
Density of donor atom N_D (cm^{-3})	1×10^{21}	1×10^{20}	1×10^{19}	0
Density of acceptor atom N_A (cm^{-3})	0	0	0	1×10^{18}
Defect density (cm^{-3})	0	0	10^{10}	10^{10}

Other than these parameters, the rest have been taken from literature [29-31]. Defect densities in the HTL and sensitizer were taken as amphoteric type with defect density of 10^{10} cm^{-2}, at an energy level of 0.6 eV with respect to the highest valence band. Interface defect densities are also added at the HTL/CTS and TiO_2/CTS interfaces which are neutral type with defect density of 10^{10} cm^{-2}, at an energy level of 0.6 eV with respect to the highest valence band. All the simulations were performed at 300 K and under standard illumination of AM 1.5G (1 Sun).

The simulations were performed using SCAPS-1D software which was developed by Prof. Marc Burglemann and his team at Gent University. The software was initially developed for the simulation of CuInGaSe (Copper Indium Gallium Selenide) and CdTe (Cadmium Telluride) thin film solar cells but it is widely used for simulation of all types of solar cells including dye sensitized and quantum dot sensitized solar cells. The simulation works by solving the Poisson's and continuity equations for electrons and holes [30]. The continuity equations for electrons and holes are as follows:

$$\frac{dJ_n}{dx} = G - R, \tag{1}$$

$$\frac{dJ_p}{dx} = G - R. \tag{2}$$

Where, Jn and Jp are the current densities of electrons and holes, G is the generation rate and R is recombination rate. The Poisson's equation is given by:

$$\frac{d^2}{dx^2}\phi(x) = \frac{q}{\varepsilon_0\varepsilon_r}\{p(x) - n(x) + N_D^+(x) - N_A^-(x) + p_t - n_t\}. \tag{3}$$

Where x indicates the distance in the solar cell, ϕ is the electrostatic potential, q is the electric charge, ε_0 is the permittivity of free space, ε_r is the relative permittivity, $p(x)$ is the concentration of free holes, $n(x)$ is the concentration of free electrons, $N_D^+(x)$ is the density of donor type charge impurities, $N_A^-(x)$ is the density of acceptor type charge impurities, p_t is the hole distribution and n_t is the electron distribution.

The simulation is done by first setting the layers of the solar cells using the "Set Problem" button where the layer parameters are given and then saved. Then "single shot calculation" is done for single simulation and "Calculate batch" for simulating a range of data. Current- Voltage curve, energy band diagram, graph of current densities, generation-recombination curves and quantum efficiency curve can be obtained after each simulation. Data on cell parameters such as the open circuit voltage (Voc), short circuit current density (Jsc), fill factor and efficiency can be obtained [32].

In the current work, an extensive evaluation is made on the defect densities of the sensitizer and hole transporting layer and their effects on the cell efficiency. Also, the effect of interface defect densities at TiO_2/CTS and CTS/HTL interfaces were also investigated. Cell efficiency was improved with the use of buffer layers of i-ZnO and CdS and the mechanism in which the cell efficiency is enhanced has also been discussed. The layer parameters of the buffer layers [27] have been tabulated in Table 2.

Table 2. Layer parameters of the buffer layers used

Buffer layer	i-ZnO	CdS
Thickness (nm)	1000	1000
Dielectric constant ($\varepsilon/\varepsilon_0$)	10	9
Electron mobility μ_e (cm^2/V_s)	50	100
Hole mobility μ_h (cm^2/V_s)	20	25
Acceptor concentration N_A (cm^{-3})	0	0
Donor concentration N_D (cm^{-3})	5×10^{17}	10^{18}
Bandgap Eg (eV)	3.4	2.4
Electron affinity (eV)	4.55	4.2
Density of state conduction band (cm^{-3})	4×10^{18}	1.8×10^{18}
Density of state valence band (cm^{-3})	9×10^{18}	2.4×10^{19}
Electron thermal velocity V_e (cms^{-1})	10^7	10^7
Hole thermal velocity V_h (cms^{-1})	10^7	10^7

3. RESULTS AND DISCUSSION

3.1. Effect of sensitizer defect density

The sensitizer defect density was varied from 10^{10}- 10^{19} cm^{-2} and the variation in efficiency has been tabulated in Table 3. There is no significant change in the efficiency of the cell except at very high defect density of 10^{19} cm^{-2}, at which the efficiency drops by 0.39%.

Table 3. Variation of efficiency with sensitizer defect density

Sensitizer defect density (cm^{-2})	Voc (V)	Jsc (mA/cm^2)	FF (%)	Efficiency (%)
10^{10}	1.034	21.04	82.14	17.86
10^{11}	1.034	21.04	82.14	17.86
10^{12}	1.034	21.04	82.14	17.86
10^{13}	1.034	21.04	82.14	17.86
10^{14}	1.034	21.04	82.14	17.86
10^{15}	1.034	21.04	82.14	17.86
10^{16}	1.034	21.04	82.14	17.86
10^{17}	1.034	21.04	82.14	17.86
10^{18}	1.034	21.04	82.14	17.85
10^{19}	1.034	21.02	81.99	17.46

The lower thickness of the sensitizer (10 nm) is one reason for the unchanged efficiency as the diffusion length of charge carriers is very less, decreasing the chance for recombination. The donor doping density of CTS is taken as 10^{19} cm^{-3} , the optimized density, which also overcomes the effect of defect levels in the sensitizer. At very high defect density, the fill factor is found to decrease which indicates the increase in series resistance in the cell, owing to more recombinations leading to comparatively lower cell efficiency. The recombination rates of charge carriers in the solar cell at various defect densities were investigated as shown in Figure 3 and it can be seen that upto defect densities of 10^{13} cm^{-2} , the recombination rate in the sensitizer is minimal, of the order of $10^{16}/cm^3s$, generation rate being $10^{22}/cm^3s$. At very high defect densities, the recombination rate in the HTL is found to decrease and that at the sensitizer is found to increase. Higher defect densities cause recombination in the sensitizer and only a few holes manage to reach the HTL, decreasing the power conversion efficiency.

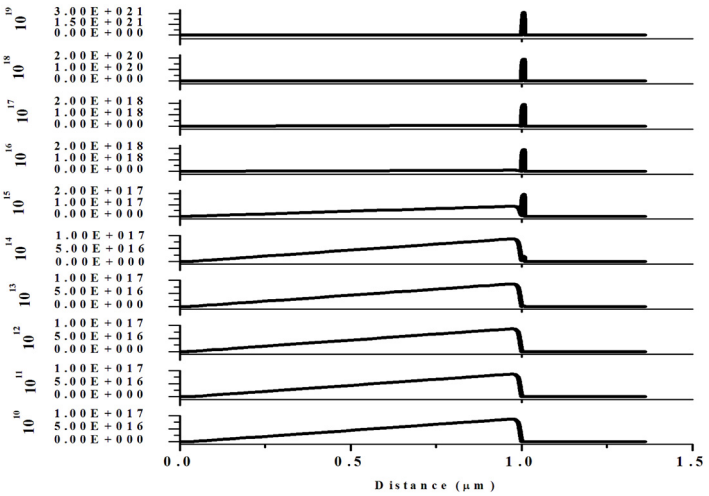

Figure 3. Recombination rates ($cm^{-3}s^{-1}$) of charge carriers at different defect densities of sensitiser

3.2. Effect of HTL defect density

Keeping the defect density of sensitizer at 10^{10} cm^{-2}, the defect density of $CuSbS_2$, the hole transporting layer was varied from 10^{10} to 10^{19} cm^{-2} and the data has been tabulated in Table 4. Here the cell efficiency is found to be independent of the defect densities except at high values of 10^{17} cm^{-2} and above. High doping density of $CuSbS_2$ is the main reason for the constancy in cell efficiency at low to moderate defect densities. At higher defect densities, Jsc is found to decrease due to increased recombination. The fill factor is also found to decrease due to increased series cell resistance owing to recombination of charge carriers and by equation 4, the cell efficiency also decreases.

$$\eta = \frac{VocJscFF}{Pin}. \quad (4)$$

Where, Voc is the open circuit voltage, Jsc is the short circuit current density, FF is the fill factor, Pin is the input power and η is the solar cell efficiency.

Table 4. Variation of cell parameters at different HTL defect densities

$CuSbS_2$ HTL defect density (cm^{-2})	Voc (V)	Jsc (mA/cm^2)	FF (%)	Efficiency (%)
10^{10}	1.034	21.04	82.14	17.86
10^{11}	1.034	21.04	82.14	17.86
10^{12}	1.034	21.04	82.14	17.86
10^{13}	1.034	21.04	82.14	17.86
10^{14}	1.034	21.04	82.14	17.86
10^{15}	1.034	20.996	82.20	17.84
10^{16}	1.035	20.594	81.17	17.30
10^{17}	1.045	18.073	74.85	14.13
10^{18}	0.742	16.091	59.73	7.13
10^{19}	0.205	0.254	25.9	0.01

3.3. Effect of interface defect density at CTS/TiO_2 interface

The interface defect density at CTS/TiO_2 interface was varied from 10^{10} to 10^{19} cm^{-2} and the data showing the variation is tabulated in Table 5. Cell efficiency was found to be independent of the defects at the CTS/TiO_2 interface.

Table 5. Variation of cell parameters at different interface defect density for CTS/TiO_2 interface

CTS/TiO_2 interface defect density (cm^{-2})	Voc (V)	Jsc (mA/cm^2)	FF (%)	Efficiency (%)
10^{10}	1.034	21.04	82.14	17.86
10^{11}	1.034	21.04	82.14	17.86
10^{12}	1.034	21.04	82.14	17.86
10^{13}	1.034	21.04	82.14	17.86
10^{14}	1.034	21.04	82.14	17.86
10^{15}	1.034	21.04	82.14	17.86
10^{16}	1.034	21.04	82.14	17.86
10^{17}	1.0335	21.006	82.02	17.81
10^{18}	1.0334	20.814	81.72	17.58
10^{19}	1.033	20.581	81.79	17.39

Figure 4 shows the band structure of the solar cell at thermodynamic equilibrium and it can be seen that there is a positive band offset between the electron transporting layer (ETL) and the sensitizer, creating a spike at the interface. The electron fermi level is seen to be close to the conduction band minimum of the sensitizer due to which there is more band bending at the interface. This spike formation at the interface acts as a barrier to the free flow of electrons hence reducing the recombination rate. Lower recombination rates at this interface unaffected the cell efficiency. At very high defect densities, the recombination rate is comparatively higher, leading to a slight drop in cell efficiency. This phenomenon is evident from the short circuit current and fill factor values which remain unchanged.

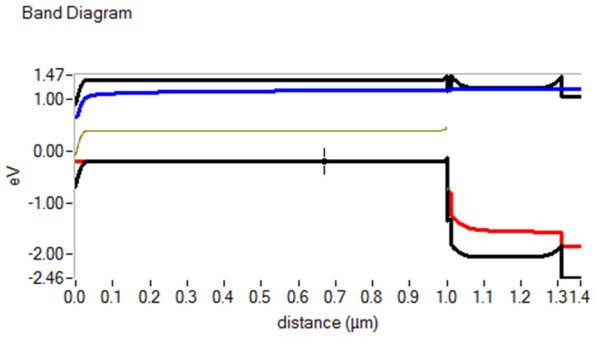

Figure 4. Band diagram of the solar cell structure at thermodynamic equilibrium

3.4. Effect of interface defect density at $CuSbS_2$/CTS interface

The defect densities at the $CuSbS_2$/CTS interface were varied from 10^{10} to 10^{14} cm^{-2} and Table 6 shows the variation in cell parameters. The cell efficiency was found to be considerably affected by the defects at this interface. The recombination rate of charge carriers of the cell at this interface has been plotted in Figure 5. The band offsets for the solar cell are conducive for the holes formed at the sensitizer to easily diffuse into the HTL. At 10^{10} and 10^{11} cm^{-2} defect densities, there is more recombination in the HTL indicating a greater number of holes reaching the HTL from the sensitizer which indicates that lesser recombinations are happening at the interface. As the defect density at the interface increases from 10^{12} to 10^{14} cm^{-2}, the recombination rate in the HTL drastically decreases signifying the drop in number of holes reaching the HTL which also signifies that more recombinations are taking place in the interface. So, at higher interface defect density at $CuSbS_2$/CTS interface, more recombinations take place at the interface, decreasing the number of holes at the electrical contacts causing the cell efficiency to significantly drop.

Table 6. Variation of cell parameters for different interface defect density at $CuSbS_2$/CTS interface

Interface defect density (cm^{-2})	Voc	Jsc	FF	Efficiency
10^{10}	1.034	21.04	82.14	17.86
10^{11}	1.0312	21.043	80.91	17.56
10^{12}	1.0078	21.043	78.34	16.61
10^{13}	0.9458	21.043	77.37	15.40
10^{14}	0.8764	21.043	76.75	14.15

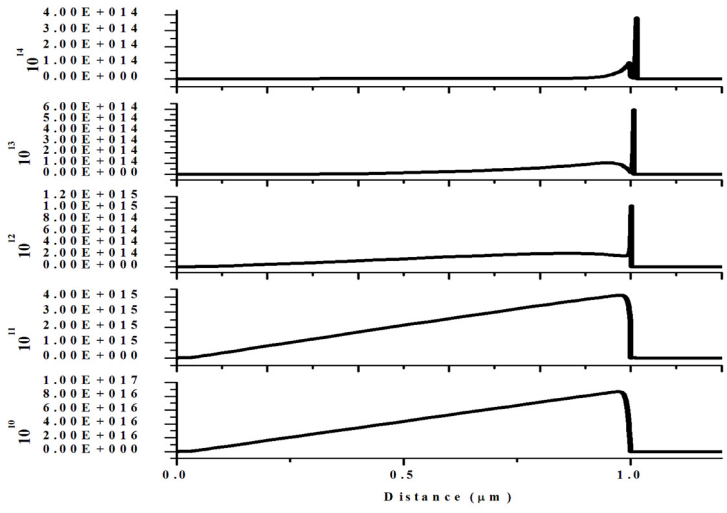

Figure 5. Recombination rate (/cm^3s) of charge carriers in the cell at varying defect densities at the $CuSbS_2$/CTS interface

3.5. Effect of buffer layer i-ZnO on the performance of CTS QDSSC

Owing to the decrease in cell efficiency due to defect densities at the CTS/HTL interface, buffer layer was used to improve the efficiency. Buffer layer of i-ZnO was inserted between the HTL and CTS sensitizer and simulations were run with different thickness of the buffer layer inorder to optimize the thickness of the buffer layer. Thickness of the buffer layer was varied from 100 nm to 1000 nm and their cell parameters were plotted as shown in Figures 6 and 7. With increasing thickness, all the cell parameters were found to increase and then saturate at 1000 nm and so the optimized thickness of i-ZnO buffer layer was taken as 1000 nm. Cell efficiency increased from 17.86% to 18.37% when this buffer layer was used.

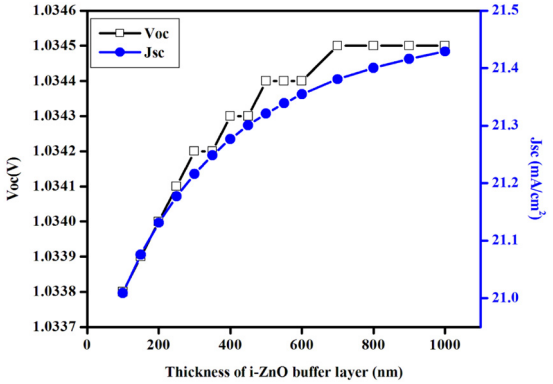

Figure 6. Variation of Voc and Jsc with increasing thickness of buffer layer

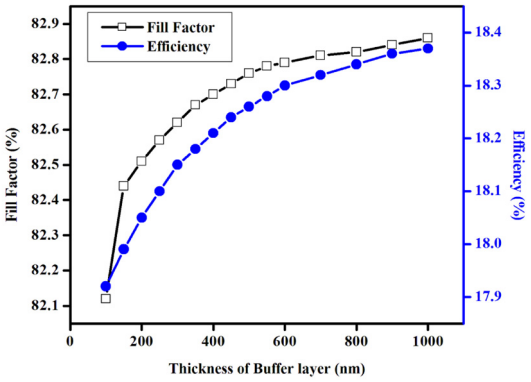

Figure 7. Variation of fill factor and efficiency with increasing thickness of buffer layer

Figure 8 shows the graph of recombination rates in the solar cell with and without the buffer layer. The recombination of charge carriers in the HTL increases by one order of magnitude when the buffer layer is used which indicates that a greater number of holes reach the HTL and there is lesser recombination at the interface. So i-ZnO is a good buffer layer which reduces the recombination at the HTL/CTS interface. The band structure of the solar cell with buffer layer has been shown in Figure 9; smooth transition of holes is possible with minimum recombination at the interfaces due to the favourable band offsets. Band structure at thermodynamic equilibrium has also been shown in Figure 10. The fermi level of electrons is found to be along the conduction band signifying higher electron density at the conduction band and higher electrical conductivity, enhancing the cell efficiency.

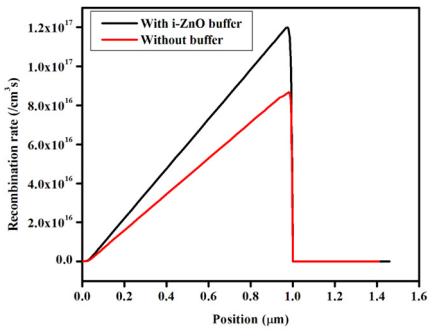

Figure 8. Recombination rates of solar cell with and without the i-ZnO buffer layer

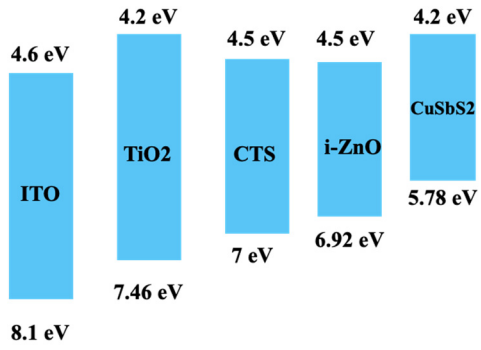

Figure 9. Band structure of the CTS QDSSC with buffer layer

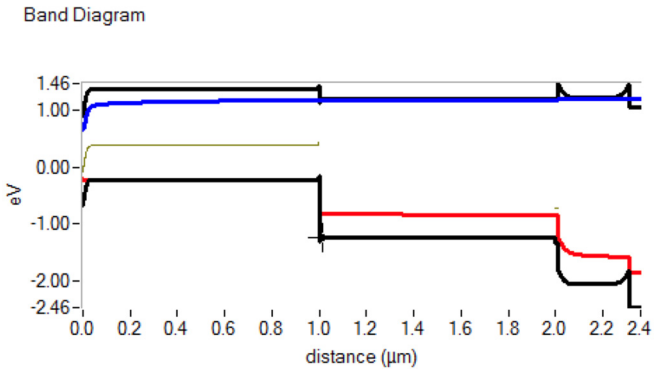

Figure 10. Band structure of the solar cell at thermodynamic equilibrium (with i-ZnO buffer)

3.6. Effect of CdS as buffer layer on the performance of CTS QDSSC

Inorder to optimise the material for buffer layer, CdS was also used in CTS QDSSC. Here too the band offsets are suitable for unhindered flow of holes and the band diagram at thermodynamic equilibrium (Figure 11) shows that the fermi level of electrons is along the conduction band facilitating electron transport and better electrical conductivity. The cell efficiency improved to 18.61% when CdS was used as a buffer layer in place of i-ZnO, the cell structure being ITO/TiO_2/CTS/CdS/$CuSbS_2$/Au. Higher fill factor was obtained as shown in Table 7, due to lower series resistance owing to lower recombination of charge carriers. The recombination rate of the solar cell with CdS buffer has been shown in Figure 12. The graph follows a gaussian curve indicating more recombination at the middle of the HTL rather than at the edges. Also, the recombination rate was found to be lower, 10^{13}(cm^{-3} s^{-1}), compared to that when i-ZnO was used. Generation of charge carriers is higher here owing to increased absorption of the solar spectrum in the high energy blue-green regime.

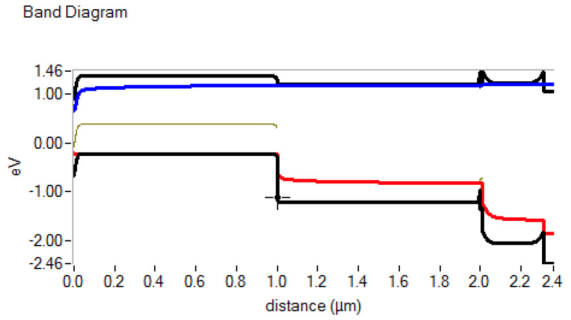

Figure 11. Energy band diagram at thermodynamic equilibrium- with CdS buffer

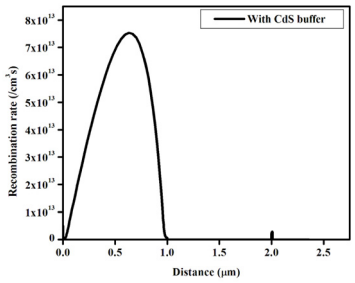

Figure 12. Recombination rate curve of solar cell when CdS is used as buffer

Table 7. Cell Parameters with CdS buffer layer

Buffer layer used	Voc (V)	Jsc (mA/cm^2)	FF (%)	Efficiency (%)
CdS	1.035	21.485	83.73	18.61

The quantum efficiency curves were plotted in all three cases, without buffer, with i-ZnO buffer and that with CdS buffer as shown in Figure 13. Absorption in the 350 nm to 500 nm is enhanced when the buffer layers are used. Solar cells with CdS buffer layer yielded higher quantum efficiency than i-ZnO, thus enhancing the cell efficiency.

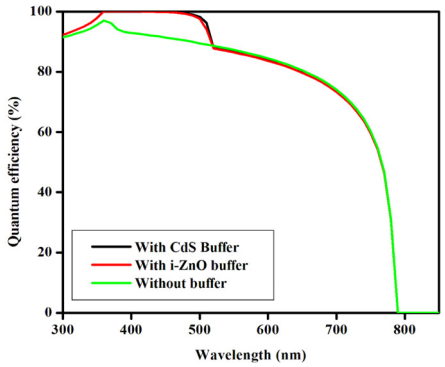

Figure 13. Quantum efficiency curves

CONCLUSIONS

Here simulation of CTS quantum dot sensitized solar cells were performed using SCAPS-1D software and an investigation was made on the effect of defects. HTL/CTS interface was found to have defects which affected the cell efficiency considerably and so buffer layers were introduced at this interface. CdS buffer layer was found to be better in performance compared to i-ZnO yielding cell efficiency of 18.61%.

Data Availability Statement

The data for the work is available with the corresponding author and can be produced upon request.

Declaration of Competing interests

The author declares that she has no known competing financial interests or personal relationships that could have appeared to influence the work reported in this paper.

Declaration of Generative AI and AI-assisted technologies in the writing process

No AI tools were used in the preparation of this manuscript.

Acknowledgements

The author would like to thank Marc Burglemann and his team for the SCAPS-1D software which is used in this work. Also, the author would like to thank Carmel College (Autonomous), Mala, Thrissur, Kerala, for the management fund for the successful completion of this work.

ORCID

Maya Mathew, https://orcid.org/0000-0002-2088-4419

REFERENCES

[1] G. Konstantatos, editor, *Colloidal quantum dot optoelectronics and photovoltaics*, (Cambridge University Press; 2013).
[2] G.H. Carey, A.L. Abdelhady, Z. Ning, S.M. Thon, O.M. Bakr, and E.H. Sargent, "Colloidal quantum dot solar cells," Chemical reviews, **115**(23), 12732-12763 (2015). https://doi.org/10.1021/acs.chemrev.5b00063
[3] I.J, Kramer, and E.H. Sargent, "Colloidal quantum dot photovoltaics: a path forward," ACS nano, **5**(11), 8506-8514 (2011). https://doi.org/10.1021/nn203438u
[4] N.M. Gabor, Z. Zhong, K. Bosnick, J. Park, and P.L. McEuen, "Extremely efficient multiple electron-hole pair generation in carbon nanotube photodiodes," Science, **325**(5946), 1367-1371 (2009). https://doi.org/10.1126/science.1176112
[5] V.I. Klimov, editor, *Nanocrystal quantum dots*, (CRC press, 2017).
[6] P.G. Prabhash, and S.S. Nair, "Synthesis of copper quantum dots by chemical reduction method and tailoring of its band gap," AIP Advances, **6**, 055003 (2016). https://doi.org/10.1063/1.4948747
[7] Sahu, A. Garg, and A. Dixit, "A review on quantum dot sensitized solar cells: Past, present and future towards carrier multiplication with a possibility for higher efficiency," Solar Energy, **203**, 210-239 (2020). https://doi.org/10.1016/j.solener.2020.04.044
[8] P. Bhambhani, "Quantum dot-sensitized solar cells: a review," Bulletin of Electrical Engineering and Informatics, **7**(1), 42-54 (2018). https://doi.org/10.11591/eei.v7i1.841
[9] T.J. Ikyumbur, F. Gbaorun, A.A. McAsule, T.M. Aper, N.S. Akiiga, A.A. Gundu, and M.S. Shiada, "SCAPS-1D simulation of a high-efficiency quantum dot solar cell using Sb_2Se_3 as an absorber layer," Next Research, **1**(2), 100084 (2024). https://doi.org/10.1016/j.nexres.2024.100084
[10] M. Mathew, and K.C. Preetha, "An exploration into the quantum confinement of CTS/natural dye core-shell quantum dots," Physica B: Condensed Matter, **579**, 411913 (2020). https://doi.org/10.1016/j.physb.2019.411913
[11] M. Mathew, and K.C. Preetha, "Effect of Pelargonidin on carrier recombination lifetime of CTS quantum dots," Optik, **205**, 164275 (2020). https://doi.org/10.1016/j.ijleo.2020.164275
[12] M. Mathew, and K.C. Preetha, "Mesoporous copper tin sulphide quantum dots as photoanode materials for efficient dye-sensitized solar cell," Optik, **224**, 165411 (2020). https://doi.org/10.1016/j.ijleo.2020.165411
[13] A.C. Lokhande, P.T. Babar, V.C. Karade, M.G. Gang, V.C. Lokhande, C.D. Lokhande, and J.H. Kim, "The versatility of copper tin sulfide," Journal of Materials Chemistry A, **7**(29), 17118-17182 (2019). https://doi.org/10.1039/C9TA00867E
[14] S. Dias, K. Kumawat, S. Biswas, and S.B. Krupanidhi, "Solvothermal synthesis of Cu_2SnS_3 quantum dots and their application in near-infrared photodetectors," Inorganic chemistry, **56**(4), 2198-2203 (2017). https://doi.org/10.1021/acs.inorgchem.6b02832
[15] S.M. Yadav, and A. Pandey, "Low Cost Solvothermal Processed CTS QDs (0D)-Based Visible-NIR Photoconductor," IEEE Sensors Journal, **21**(18), 19978-19983 (2021). https://doi.org/10.1109/JSEN.2021.3099059
[16] Y. Chen, L. Ma, Y. Yin, X. Qian, G. Zhou, X. Gu, W. Liu, *et al*., "Strong quantum confinement effect in Cu_4SnS_4 quantum dots synthesized via an improved hydrothermal approach," Journal of Alloys and Compounds, **5**(672), 204-211 (2016). https://doi.org/10.1016/j.jallcom.2016.02.135
[17] V. Maheskumar, and B. Vidhya, "Investigation on the morphology and photocatalytic activity of Cu_3SnS_4 synthesized by ball milling and solvothermal method," Journal of Photochemistry and Photobiology A: Chemistry, **356**, 521-529 (2018). https://doi.org/10.1016/j.jphotochem.2017.12.026
[18] V. Maheskumar, I. Sheebha, B. Vidhya, J.P. Deebasree, T. Selvaraju, and S. Akash, "Enhanced electrocatalytic and photocatalytic activity of ball milled copper tin sulphide by incorporating GO and rGO," Applied Surface Science, **484**, 265-275 (2019). https://doi.org/10.1016/j.apsusc.2019.03.241
[19] S. Rühle, M. Shalom, and A. Zaban, "Quantum-dot-sensitized solar cells," ChemPhysChem. **11**(11), 2290-2304 (2010). https://doi.org/10.1002/cphc.201000069
[20] S. Emin, S.P. Singh, L. Han, N. Satoh, and A. Islam, "Colloidal quantum dot solar cells," Solar Energy, **85**(6), 1264-1282 (2011). https://doi.org/10.1016/j.solener.2011.02.005
[21] X. Ma, X. Yang, M. Wang, R. Qin, D. Xu, C. Lan, K. Zhao, *et al*., "Comprehensive Passivation on Different Charged Ions and Defects for High Efficiency and Stable Perovskite Solar Cells," Advanced Energy Materials, **15**(3), 2402814 (2025). https://doi.org/10.1002/aenm.202402814
[22] Z. Yang, Y. Liu, and W. Chen, "A brief review of perovskite quantum dot solar cells: Synthesis, property and defect passivation," ChemSusChem. **18**(3), e202401587 (2025). https://doi.org/10.1002/cssc.202401587
[23] T.K. Nideep, M. Ramya, and M. Kailasnath, "The influence of ZnS buffer layer on the size dependent efficiency of CdTe quantum dot sensitized solar cell," Superlattices and Microstructures, **130**, 175-181 (2019). https://doi.org/10.1016/j.spmi.2019.04.034
[24] Manjceevan, and J. Bandara, "Systematic stacking of PbS/CdS/CdSe multi-layered quantum dots for the enhancement of solar cell efficiency by harvesting wide solar spectrum," Electrochimica Acta, **271**, 567-575 (2018). https://doi.org/10.1016/j.electacta.2018.03.193
[25] M.A. Basit, M.A. Ali, Z. Masroor, Z. Tariq, and J.H. Bang, "Quantum dot-sensitized solar cells: a review on interfacial engineering strategies for boosting efficiency," Journal of Industrial and Engineering Chemistry, **120**, 1-26 (2023). https://doi.org/10.1016/j.jiec.2022.12.016
[26] E. Laghchim, A. Raidou, A. Fahmi, and M. Fahoume, "The effect of ZnS buffer layer on Cu_2SnS_3 (CTS) thin film solar cells performance: numerical approach," Micro and Nanostructures, **165**, 207198 (2022). https://doi.org/10.1016/j.micrna.2022.207198

[27] Z.R. Abdulghani, A.S. Najm, A.M. Holi, A.A. Al-Zahrani, K.S. Al-Zahrani, and H. Moria, "Numerical simulation of quantum dots as a buffer layer in CIGS solar cells: A comparative study. Scientific Reports, **12**(1), 8099 (2022). https://doi.org/10.1038/s41598-022-12234-0
[28] T.K. Nideep, M. Ramya, and M. Kailasnath, "The influence of ZnS buffer layer on the size dependent efficiency of CdTe quantum dot sensitized solar cell," Superlattices and Microstructures, **130**, 175-181 (2019). https://doi.org/10.1016/j.spmi.2019.04.034
[29] Siddique, M.N. Islam, H. Karmaker, A.A. Iqbal, A.A. Khan, M.A. Islam, and B.K. Das, "Numerical modelling and performance investigation of inorganic Copper-Tin-Sulfide (CTS) based perovskite solar cell with SCAPS-1D," Results in Optics, **16**, 100713 (2024). https://doi.org/10.1016/j.rio.2024.100713
[30] E. Danladi, P.M. Gyuk, N.N. Tasie, A.C. Egbugha, D. Behera, I. Hossain, I.M. Bagudo, et al., "Impact of hole transport material on perovskite solar cells with different metal electrode: a SCAPS-1D simulation insight," Heliyon, **9**(6), e16838 (2023). https://doi.org/10.1016/j.heliyon.2023.e16838
[31] S. Kumar, P. Bharti, and B. Pradhan, "Performance optimization of efficient PbS quantum dots solar cells through numerical simulation," Scientific Reports, **13**(1), 10511 (2023). https://doi.org/10.1038/s41598-023-36769-y
[32] M. Burgelman, K. Decock, A. Niemegeers, J. Verschraegen, and S. Degrave, *SCAPS manual*, (University of Ghent, Ghent, Belgium, 2016).

БУФЕРНІ ШАРИ i-ZnO І CdS ДЛЯ ПІДВИЩЕННЯ ЕФЕКТИВНОСТІ СОНЯЧНИХ ЕЛЕМЕНТІВ, СЕНСИБІЛІЗОВАНИХ КВАНТОВИМИ ТОЧКАМИ СУЛЬФІДУ МІДІ ТА ОЛОВА

Майя Метью

Факультет фізики, Кармел коледж, (автономний), Мала, Тріссур, Керала, Індія

Вплив дефектів шару, а також дефектів інтерфейсу в сонячних елементах, чутливих до квантових точок із сульфіду міді та олова, досліджували за допомогою програмного забезпечення SCAPS-1D. Було виявлено, що дефекти шару сенсибілізатора та шару транспортування дірок не впливають на ефективність клітини, за винятком дуже високих щільностей 10^{19} $см^{-2}$. Було також виявлено, що дефект інтерфейсу в CTS/ETL не впливає на ефективність клітинки. Дефекти на інтерфейсі HTL/CTS значно знизили ефективність комірки, тому на цьому інтерфейсі було введено буферний шар. Було виявлено, що і матеріали буферного шару i-ZnO, і CdS мають рівні енергії, узгоджені з HTL, що посилює транспортування заряду. Ефективність елемента зросла з 17,86% до 18,37% з буферним шаром i-ZnO, тоді як ефективність елемента зросла до 18,61% при використанні CdS як буферного шару. Поглинання сонячного спектру в синьо-зеленій області посилювалося при використанні в комірці буферних шарів.

Ключові слова: *сенсибілізовані квантовими точками сонячні елементи; буферний шар; SCAPS-1D; рекомбінація носіїв заряду; квантова ефективність; дефекти*